

## Kinetic Analysis of the Zinc-Dependent Deacetylase in the Lipid A Biosynthetic Pathway<sup>†</sup>

Amanda L. McClerren, Pei Zhou, Ziqiang Guan, Christian R. H. Raetz, and Johannes Rudolph\*

Department of Biochemistry, Duke University Medical Center, P.O. Box 3813, Durham, North Carolina 27710

Received September 16, 2004; Revised Manuscript Received October 19, 2004

**ABSTRACT:** The first committed step of lipid A biosynthesis in Gram-negative bacteria is catalyzed by the zinc-dependent hydrolase LpxC that removes an acetate from the nitrogen at the 2''-position of UDP-3-O-acyl-N-acetylglucosamine. Recent structural characterization by both NMR and X-ray crystallography provides many important details about the active site environment of LpxC from *Aquifex aeolicus*, a heat-stable orthologue that displays 32% sequence identity to LpxC from *Escherichia coli*. The detailed reaction mechanism and specific roles of active site residues for LpxC from *A. aeolicus* are further analyzed here. The pH dependencies of  $k_{\text{cat}}/K_M$  and  $k_{\text{cat}}$  for the deacetylation of the substrate UDP-3-O-[(R)-3-hydroxymyristoyl]-GlcNAc are both bell-shaped. The ascending acidic limb ( $\text{p}K_1$ ) was fitted to  $6.1 \pm 0.2$  for  $k_{\text{cat}}$  and  $5.7 \pm 0.2$  for  $k_{\text{cat}}/K_M$ . The descending basic limb ( $\text{p}K_2$ ) was fitted to  $8.0 \pm 0.2$  for  $k_{\text{cat}}$  and  $8.4 \pm 0.2$  for  $k_{\text{cat}}/K_M$ . The pH dependence of the E73A mutant exhibits loss of the acidic limb, and the mutant retains only 0.15% activity versus the wild type. The pH dependencies of the other active site mutants H253A, K227A, H253A/K227A, and D234N remain bell-shaped, although their significantly lower activities (0.25%, 0.05%, 0.007%, and 0.57%, respectively) suggest that they contribute significantly to catalysis. Our cumulative data support a mechanism for LpxC wherein Glu73 serves as the general base for deprotonation and activation of the zinc-bound water.

Lipopolysaccharide (LPS)<sup>1</sup> is a unique glycolipid found at the cell surface of most Gram-negative bacteria, including *Escherichia coli* and *Salmonella typhimurium*. LPS is an important immunogenic determinant of Gram-negative bacterial infections and provides a formidable barrier to many potentially bactericidal compounds and environmental hazards. Lipid A is the hydrophobic anchor moiety of LPS, securing it to the outer surface of the outer membrane. Lipid A is a hexaacylated  $\beta(1'–6)$ -linked disaccharide of glucosamine that is glycosylated with two 3-deoxy-D-manno-octulosonic acid (Kdo) sugars at position 6' to comprise the minimal structure of LPS required for growth in most Gram-negative bacteria (1).

The biosynthetic pathway of lipid A is conserved and involves nine essential enzymes. The second of these is LpxC, a deacetylase that removes acetate from the nitrogen at the 2''-position of UDP-3-O-acyl-N-acetylglucosamine. Because the first step of biosynthesis is thermodynamically unfavorable, deacetylation by LpxC is the first committed step of the pathway, making LpxC an attractive target for antibiotic design. LpxC, like other zinc-dependent hydrolases, can be effectively inhibited by hydroxamate-containing

compounds (2–5). One of these is TU-514, a substrate-analogue inhibitor of LpxC that binds to the active site  $\text{Zn}^{2+}$ . TU-514 is the only compound known to inhibit a broad range of LpxC orthologues, showing potency against LpxC from both *E. coli* and *Aquifex aeolicus*, the latter orthologue having only 32% sequence identity with the one from *E. coli* (3). However, TU-514 lacks efficacy in vivo, most likely because it is excluded by the cell envelope. Progress in the development of more effective inhibitors of this important target may be facilitated by a better understanding of the catalytic mechanism of LpxC.

Recently, the structure of LpxC from *A. aeolicus* was determined by NMR (6) and X-ray crystallography (7). The protein consists of two domains with similar folds, each containing a layer of  $\alpha$ -helices packing against a primary  $\beta$ -sheet. LpxC contains a novel  $\text{Zn}^{2+}$ -binding motif, HKXXD, with  $\text{Zn}^{2+}$  coordination by His74, His226, and Asp230 (Figure 1). A water molecule serves as the fourth ligand in the free enzyme but can be replaced by the carbonyl oxygen of the hydroxamate in the inhibitor-bound structure. Conserved Lys227 could function to stabilize the transition state or organize the active site. Conserved residues Glu73 and His253 are also located in the active site and have been shown to coordinate a second inhibitory  $\text{Zn}^{2+}$  ion present in the crystal structure. Additionally, these two residues may be in position to hydrogen bond to the substrate or zinc-bound water molecule. Asp234 is also conserved and is located one helical turn away from the  $\text{Zn}^{2+}$  ligand Asp230, within H-bonding distance to His253 (Figure 1).

Although LpxC shows no amino acid sequence homology with other known zinc-dependent hydrolases and has a

<sup>†</sup> This research was supported by NIH Grant GM-51310 to C.R.H.R. and NIH AI-055588 to P.Z. The mass spectrometry facility in the Department of Biochemistry of the Duke University Medical Center and Z.G. were supported by the LIPID MAPS Large Scale Collaborative Grant number GM069338 from NIH.

\* To whom correspondence should be addressed. Phone: (919) 668-6188. Fax: (919) 613-8642. E-mail: rudolph@biochem.duke.edu.

<sup>1</sup> Abbreviations: LPS, lipopolysaccharide; UDP-GlcNAc, UDP-N-acetylglucosamine; UDP-3-O-acyl-GlcNAc, UDP-3-O-acyl-N-acetylglucosamine; BSA, bovine serum albumin.

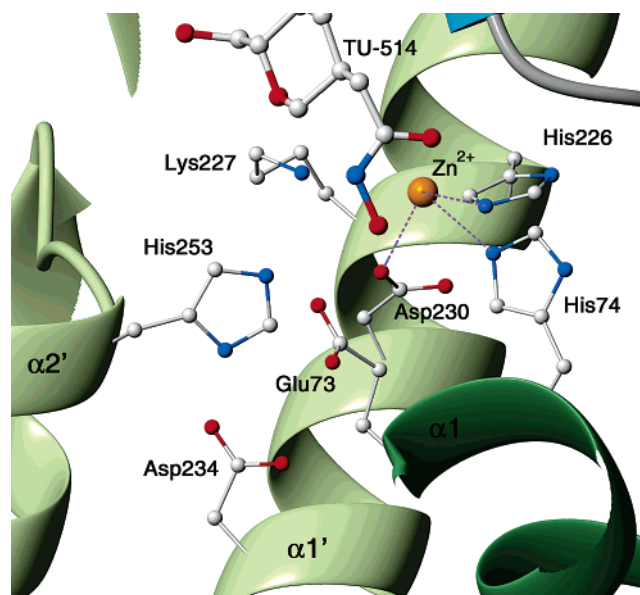


FIGURE 1: Active site region of *A. aeolicus* LpxC with TU-514 bound from the refined NMR structure (following paper in this issue). The  $Zn^{2+}$  is coordinated by His74, His226, and Asp230. The figure was prepared using MOLMOL software (39).

different protein fold, its active site is similar to those of well-studied zinc-dependent hydrolases such as thermolysin, carboxypeptidase A, and matrilysin (8–11).  $Zn^{2+}$  coordination in these proteins generally occurs through three protein residues, 2–3 histidines and 0–1 carboxylate provided by an aspartate or glutamate. The fourth ligand is a bound solvent molecule that can be displaced by substrate analogues or inhibitors. The mechanisms of these well-studied zinc-dependent hydrolases share several common features.  $Zn^{2+}$  polarizes a bound water molecule, activating it for nucleophilic attack on the carbonyl carbon of the substrate. This activation may also require the assistance of a general base, usually a glutamate, which abstracts a proton from the water. Additionally, the  $Zn^{2+}$  ion is thought to polarize the carbonyl of the substrate, thus making it more susceptible to nucleophilic attack by the activated water molecule. The resulting tetrahedral oxyanion intermediate is stabilized by one or more hydrogen bonds to other active site residues and potential coordination to the  $Zn^{2+}$ . Collapse of the tetrahedral intermediate requires donation of a proton to the amide nitrogen to facilitate the departure of the leaving group. The glutamate that formerly acted as a general base may now be in a position to donate this proton. In addition, the identity and specific roles of the  $Zn^{2+}$  ligands and adjacent amino acid groups show variability among the zinc-dependent hydrolases.

Given the importance of LpxC in LPS biosynthesis, we set out to investigate the reaction mechanism in more detail. The visualization of the active site residues by recent structural efforts led to two proposed catalytic mechanisms for this enzyme (6, 7). The zinc-bound water coordinated to His74, His226, and Asp230 forms the basis for both mechanisms. The major difference arises in the identity of the general base. The proximity of Glu73 ( $\sim 4.5$  Å) to the  $Zn^{2+}$  in the crystal structure, as well as precedence from carboxypeptidase A and thermolysin, suggested that this residue serves as the catalytic base (7). On the other hand, the E73A mutant has been shown to retain significant activity

in cell extracts ( $\sim 10\%$ ) (6, 12), and the position of His253 ( $\sim 4.5$  Å to the  $Zn^{2+}$ ) predicted by the NMR structure suggested that His253 might act as the general base. Supporting this proposal, the H253A and H253Q mutants appeared to have no residual activity when assayed in cell extracts (6, 12), and a similar role for histidine has been proposed in a histone deacetylase homologue (13). The two mechanisms also vary in the residues predicted to support catalysis through hydrogen bonding and stabilization of the oxyanion intermediate (Figure 2). Herein we have characterized the mechanism of LpxC by measuring the pH dependence of the deacetylase reaction with wild-type enzyme and several site-directed mutants of residues expected to contribute to catalysis.

## MATERIALS AND METHODS

**Buffers and Reagents.** [ $\alpha$ - $^{32}P$ ]UTP was purchased from NEN Dupont. PEI-cellulose TLC plates were purchased from EMD Chemicals. Bovine serum albumin (BSA), sodium acetate, bis-Tris, and Tris buffers were purchased from Sigma. Primers were purchased from MWG Biotech. All other reagents were of high commercial grade.

**Site-Directed Mutagenesis.** Site-directed mutants K227A and K227A/H253A of LpxC were prepared using the QuikChange site-directed mutagenesis kit (Stratagene). The E73A, H253A, and D234N substitutions have been described previously (12). Primers for the K227A mutation were 5'-aac gaa cct gta aga cac GCG gtg ttt gac ctt ata gga and 3'-tcc tat aag gtc aaa cac CGC gtg tct tac agg ttc gtt. Constructs were confirmed by DNA sequencing and ESI mass spectrometry of the purified proteins. Mass spectra were acquired on a QSTAR XL quadrupole time-of-flight tandem mass spectrometer (ABI/MDS-Sciex, Toronto, Canada) equipped with an electrospray source. Purified proteins dissolved in water/acetonitrile/formic acid (49:49:2, v/v) at a concentration of  $\sim 10$   $\mu$ M were infused at a flow rate of 10  $\mu$ L/min and electrosprayed at 4.5 kV. Data acquisition and analysis were performed using the instrument's Analyst QS software.

**Purification of Wild-Type *A. aeolicus* LpxC and Site-Directed Mutants.** Plasmids of each construct were transformed into BLR(DE3)-pLysS for overexpression and purification. Overnight cultures were grown in LB broth containing 100  $\mu$ g/mL ampicillin and 25  $\mu$ g/mL chloramphenicol at 37 °C and used to inoculate 1 L cultures of LB broth containing the same antibiotics. These cultures were grown with shaking at 37 °C until  $A_{600}$  reached 0.4–0.5. Cultures were then induced with addition of 1 mM IPTG and 100  $\mu$ M  $ZnSO_4$ , and grown for 5.5 h at 20 °C. Cells were harvested by centrifugation, and cell pellets were frozen overnight at  $-80$  °C. Once thawed, the pellets were resuspended in 10 volumes of 25 mM sodium phosphate buffer (pH 7) containing 100 mM KCl and 2 mM DTT. The cells were lysed by one passage through a French pressure cell at 18 000 psi, and the membranes were removed by ultracentrifugation for 1 h at 45 000 rpm. The extracts were then diluted 5-fold into 25 mM HEPES, pH 7, containing 2 mM DTT. LpxC variants were purified using anion-exchange (50 mL or larger Q-sepharose fast flow, Amersham, 0–350 mM KCl) and size-exclusion (320 mL or larger Sephacryl S-200 HR, Amersham) chromatography. The samples were concentrated to at least 1.5 mg/mL protein and stored at  $-80$

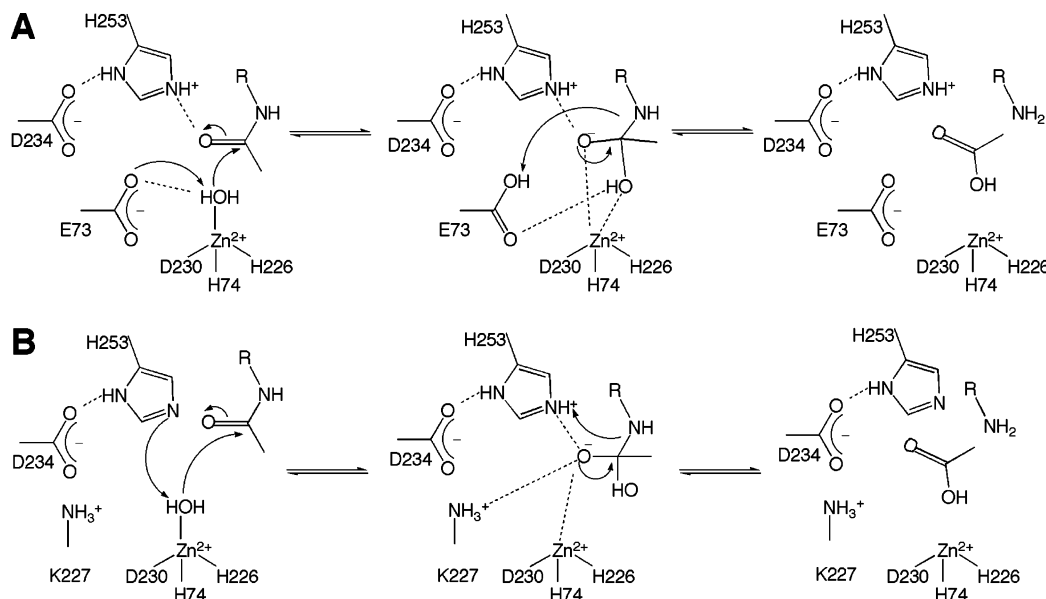


FIGURE 2: Proposed catalytic mechanisms for LpxC. (A) Glu73 acts as the general base to activate water for nucleophilic attack at the scissile amide linkage of the substrate. The tetrahedral intermediate is stabilized by His253 (7). (B) His253 acts as the general base to activate water for nucleophilic attack at the carbonyl carbon of the substrate. The oxyanion intermediate is stabilized by Lys227 (6).

°C in 25 mM sodium phosphate buffer (pH 7) containing 150 mM KCl and 2 mM DTT.

**LpxC Activity Assays.** Rates of LpxC-catalyzed deacetylation were measured for the substrate UDP-3-*O*-[(*R*)-3-hydroxymristoyl]-*N*-acetylglucosamine, prepared as previously described (14). Both <sup>32</sup>P-labeled and nonradioactive carrier substrates were prepared. The specific activity of the radioactive substrate used varied from 200 000 to 5 000 000 cpm/nmol. Wild-type LpxC and the variants were assayed in a three-component buffer system containing 100 mM sodium acetate, 50 mM bis-Tris, and 50 mM Tris across a pH range of 4–9.5. The pH's of the buffers were routinely checked under mock assay conditions at 50 °C and adjusted accordingly. All reaction mixtures contained 1 mg/mL BSA. Assays were performed at 50 °C in a heat block. Reaction mixtures containing all assay components except enzyme were preincubated for 3 min prior to the start of the assay. LpxC dilutions were made in 1 mg/mL BSA and the three-component assay buffer at the pH for each given reaction. Enzyme dilutions were stored on ice until dilution into the final assay mixture to initiate the reaction (5  $\mu$ L into 20  $\mu$ L). The substrate concentration was varied from 0.2 $K_M$  to 5 $K_M$  (1–25  $\mu$ M) for the complete  $K_M$  determinations. For the  $k_{cat}/K_M$  studies, substrate (1 or 2  $\mu$ M) and enzyme concentrations were varied to ensure adherence to  $k_{cat}/K_M$  conditions. For the  $V_{max}$  studies, assays were performed at a substrate concentration of 5 $K_M$  (25  $\mu$ M). Reaction samples (5  $\mu$ L) were removed at specific time points and quenched with 1  $\mu$ L of 1.25 M NaOH. Further incubation at 30 °C for 10 min fully deacylated both substrate and product, yielding <sup>32</sup>P-labeled UDP-glucosamine or UDP-GlcNAc. Addition of 1  $\mu$ L of 1.25 M acetic acid neutralized the samples. BSA was precipitated by addition of 1  $\mu$ L of 5% TCA, followed by incubation on ice for 5 min and centrifugation for 3 min. Samples were then spotted (1  $\mu$ L) on PEI-cellulose TLC plates (5000–25000 cpm/sample) which were developed in 0.2 M guanidine hydrochloride. The plates were exposed to Phosphor-Imaging screens overnight and quantified using a Phosphor-Imager and ImageQuant software. All assays were performed

in duplicate or quadruplicate, and product formation (<10% overall conversion) was linear over the time course of the assay.

Steady-state kinetic parameters  $k_{cat}/K_M$  and  $k_{cat}$  and standard errors for LpxC activity were determined by a fit of initial velocities to the Michaelis–Menten equation using Microsoft Excel software (15). The pH-dependent ionizations were determined by a fit of steady-state parameters to eq 1 or 2, wherein  $v$  is the observed rate of the reaction,  $C$  is the pH-independent rate,  $[H]$  is the concentration of hydrogen ions, and  $K_a$  and  $K_b$  reflect the ionization constants of the acid and base species, respectively (16).

$$v = \frac{C}{1 + [H]/K_a + K_b/[H]} \quad (1)$$

$$v = \frac{C}{1 + K_b/[H]} \quad (2)$$

## RESULTS AND DISCUSSION

**pH Dependence of Wild-Type LpxC.** The pH dependence of *A. aeolicus* LpxC was measured with the substrate UDP-3-*O*-acyl-*N*-acetylglucosamine (UDP-3-*O*-acyl-GlcNAc). Because of the precedence of altered reaction mechanisms for zinc-dependent hydrolases with artificial substrates (10, 17–20) and the low activity of LpxC from *E. coli* with UDP-GlcNAc (14), the use of a natural substrate was deemed essential. The substrate has no ionizable groups in the pH range tested. Although the optimal growth temperature of *A. aeolicus* is 70–80 °C, assays of LpxC were performed at 50 °C to limit evaporation. Our three-component buffer system covered the pH range of 4.0–9.5.

The pH dependencies of the kinetic parameters  $k_{cat}/K_M$  and  $k_{cat}$  are shown in Figure 3. The second-order rate constant  $k_{cat}/K_M$  describes the kinetic events between the free enzyme and free substrate, from substrate binding up to and including the first irreversible step. On the other hand, the rate constant  $k_{cat}$  describes the rate-limiting events of the overall reaction.

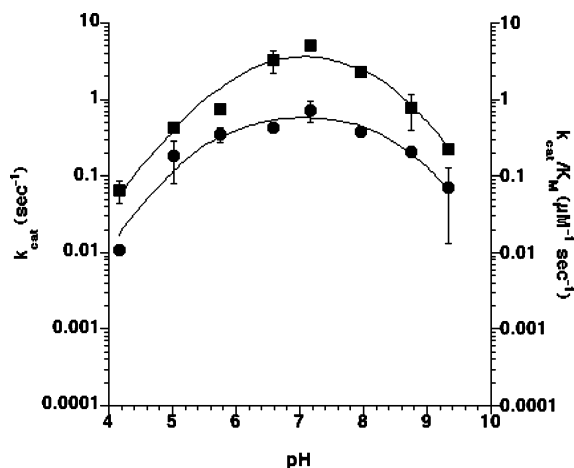


FIGURE 3: pH dependence of kinetic parameters  $k_{\text{cat}}/K_M$  and  $k_{\text{cat}}$  for wild-type LpxC. Closed squares represent  $k_{\text{cat}}$ , and closed circles represent  $k_{\text{cat}}/K_M$ .

Table 1

protein	$pK_1$	$pK_2$	type of experiment
wild type	$6.1 \pm 0.2$	$8.0 \pm 0.2$	$k_{\text{cat}}$
wild type	$5.5 \pm 0.2$	$8.4 \pm 0.2$	$k_{\text{cat}}/K_M$
wild type	$5.4 \pm 0.1$	$8.4 \pm 0.1$	$V_{\text{max}}$
E73A	none	$7.5 \pm 0.1$	$V_{\text{max}}$
H253A	$5.8 \pm 0.1$	$8.0 \pm 0.1$	$V_{\text{max}}$
K227A	$5.9 \pm 0.1$	$7.8 \pm 0.1$	$V_{\text{max}}$
K227A/H253A	$5.5 \pm 0.1$	$8.0 \pm 0.2$	$V_{\text{max}}$
D234N	$5.5 \pm 0.2$	$7.3 \pm 0.2$	$V_{\text{max}}$

For the LpxC reaction, assuming no rate-limiting conformational changes, both  $k_{\text{cat}}/K_M$  and  $k_{\text{cat}}$  are expected to be determined by the essentially irreversible attack of water and loss of acetate. The individual kinetic parameters were determined by fitting to data from complete  $K_M$  determinations, varying [UDP-3-*O*-acyl-GlcNAc] from  $0.2K_M$  to  $5K_M$ . The bell-shaped profiles of both  $k_{\text{cat}}/K_M$  and  $k_{\text{cat}}$  are characteristic of two ionization events in the reaction. The acidic limb of the bell-shaped profile shows an ionization with a  $pK_1 = 6.1 \pm 0.2$  for  $k_{\text{cat}}$  and  $5.7 \pm 0.2$  for  $k_{\text{cat}}/K_M$  (Table 1). The basic limb of the profile exhibits an ionization with  $pK_2 = 8.0 \pm 0.2$  for  $k_{\text{cat}}$  and  $8.4 \pm 0.2$  for  $k_{\text{cat}}/K_M$  (Table 1). As expected by the similarity between the  $k_{\text{cat}}/K_M$  and  $k_{\text{cat}}$  profiles,  $K_M$  values are independent of pH, ranging from 4 to  $6 \mu\text{M}$  (data not shown). The similarity of the pH-rate profiles for  $k_{\text{cat}}$  and  $k_{\text{cat}}/K_M$  suggests that the pH dependence of the LpxC reaction is defined by  $k_{\text{cat}}$ . This result indicates that the pH-dependent ionizations do not involve substrate binding, instead reflecting chemistry involved in the reaction. This interpretation is supported by the absence of burst kinetics at high enzyme concentrations that would indicate a rate-determining step such as product release following chemistry (data not shown). In addition, neither ionization is the result of buffer catalysis since varying the concentration of Tris base in the assay from 25 to 100 mM at constant ionic strength at pH 7.5 did not affect the reaction rate (data not shown). The  $pK_1$  and  $pK_2$  values therefore likely describe ionization events in the active site required for catalysis.  $pK_1$  reflects a group whose deprotonation is required for efficient catalysis, while  $pK_2$  represents a group that is protonated during catalysis. Specifically for LpxC (Figure 2),  $pK_1 \approx 6$  most likely represents the general base. The role of the group

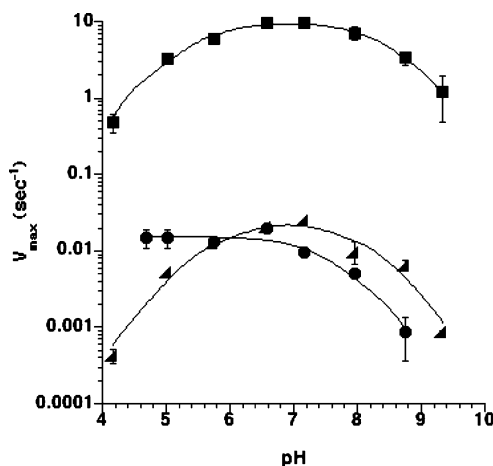


FIGURE 4: pH dependence of  $V_{\text{max}}$  for the E73A (circles) and H253A (triangles) mutants of LpxC. The pH dependence for the wild-type enzyme (squares) is shown for comparison.

with  $pK_2 \approx 8$  is less certain in the mechanism. Most intuitively it acts as a hydrogen bond donor to stabilize the oxyanion of the tetrahedral intermediate, much like the conserved arginine in carboxypeptidase A (21). Alternatively,  $pK_2$  could be measuring the protonation state of the zinc-bound water since  $pK_a$  values of this species can vary between 8 and 10 (22–24). Finally,  $pK_2$  may reflect a more subtle organization of the active site in the Michaelis complex. Importantly, neither  $pK_1$  nor  $pK_2$  is expected to be associated with the three  $\text{Zn}^{2+}$  ligands His74, His226, and Asp230.

*pH Dependence of mutants E73A and H253A.* Given the two previously proposed mechanisms (Figure 2), the site-directed mutants E73A and H253A were purified and their pH-dependent activity was determined to test which residue serves the role as catalytic base with a  $pK_a \approx 6$ . Because of the low residual activity of these mutants (see below), their purity is of particular importance, especially the potential contamination by LpxC from *E. coli*. In addition to SDS-PAGE analysis (data not shown), we have used ESI-MS (Supporting Information Figure 1) to demonstrate the high purity of our enzyme preparations. Due to the difficulty in performing  $K_M$  experiments in mutants with greatly reduced activity, pH-rate profiles were initially performed under  $V_{\text{max}}$  conditions ([UDP-3-*O*-acyl-GlcNAc] = 25 or  $50 \mu\text{M} = 5K_M$  or  $10K_M$ ) for each mutant and wild-type at  $50^\circ\text{C}$ . Essentially identical rates at these two saturating substrate concentrations were obtained at each pH and are analogous to  $V_{\text{max}}$ , from which the  $k_{\text{cat}}$  term can be extrapolated. Since we have shown that  $K_M$  for the wild type is independent of pH and assuming the mutations do not affect substrate binding, the  $V_{\text{max}}$  profiles for each mutant reflect  $k_{\text{cat}}$  and can be compared to that of the wild type. Alterations in the pH profiles of  $V_{\text{max}}$  can then be investigated further using complete  $K_M$  determinations or more limited  $k_{\text{cat}}/K_M$  measurements. As expected from the  $k_{\text{cat}}/K_M$  and  $k_{\text{cat}}$  profiles, the  $V_{\text{max}}$  profile of wild-type LpxC exhibits a bell-shaped pH dependence with  $pK_1 = 5.4 \pm 0.1$  and  $pK_2 = 8.4 \pm 0.1$  (Figure 4, Table 1).

In contrast, the activity of E73A is no longer pH-dependent at acidic pH, resulting in loss of the acidic limb of the bell-shaped profile and leaving only a single pH-dependent ionization with  $pK_2 = 7.5 \pm 0.1$  (Figure 4, Table 1). Additionally, the pH-dependent  $V_{\text{max}}$  activity is 0.15% of that

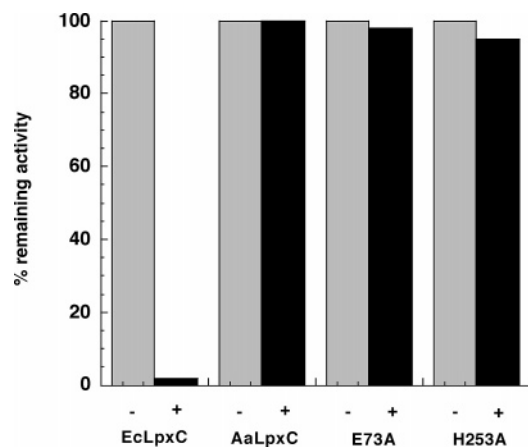


FIGURE 5: Inhibition of LpxC enzymes by L-161,240. EcLpxC is wild-type LpxC from *E. coli*, AaLpxC is wild-type LpxC from *A. aeolicus*, and E73A or H253A are site-directed mutants from *A. aeolicus*. Percent activities for each enzyme were determined by normalizing the reaction containing 1  $\mu\text{g/mL}$  inhibitor (black bar) against a reaction containing no inhibitor (gray bar).

of the wild type, and this mutant is not stable at pH extremes less than 4.5 or greater than 9.0. The low residual activity for the E73A mutant differs from the 10% residual activity previously reported (6, 12). Part of the discrepancy comes from the pH of the previous assays being 5.5, where the E73A mutant is more active compared to the wild type than for the pH-independent values derived from eq 1 or 2. Using the previous purification procedure, contamination of the E73A mutant by wild-type LpxC from *E. coli* may also have contributed to the apparent higher activity. We have ensured that the residual activities of the E73A and H253A mutants are free from this potential contamination by assaying in the presence of 1  $\mu\text{g/mL}$  L-161,240, a specific inhibitor of LpxC from *E. coli* (3, 5). Under these conditions, LpxC from *E. coli* is inhibited completely (Figure 5). In contrast, the activities of the wild type, E73A, and H253A proteins from *A. aeolicus* were unaffected by the addition of inhibitor, confirming the reactive purity of the samples. The large decrease in activity and change in pH dependence seen in E73A is due to alterations in  $k_{\text{cat}}$  alone. The  $K_M$  of E73A remains pH-independent from pH 4.5 to pH 9.5, although it is  $\sim 3$ -fold lower than that of the wild type (1–3  $\mu\text{M}$ , data not shown). In contrast to E73A, the H253A mutant did not show a greatly altered pH-dependent  $V_{\text{max}}$  profile (Figure 4). Although the activity of H253A was also only 0.25% of that of the wild type,  $\text{p}K_1 = 5.8 \pm 0.1$  and  $\text{p}K_2 = 8.0 \pm 0.1$  are very similar to those of the wild-type protein (Table 1). The  $K_M$  of this mutant remains pH-independent as well, since pH-dependent assays performed under  $k_{\text{cat}}/K_M$  conditions (1–2  $\mu\text{M}$  substrate) at pH 4, 7.2, or 8.8 indicate a bell-shaped profile with similar inflection points (data not shown).

The specific loss of the acidic limb for the E73A mutant is most consistent with the assignment of Glu73 as the catalytic base (Figure 2). This interpretation is in agreement with the proposed mechanism in which Glu73 acts a general base to activate the zinc-bound water for nucleophilic attack at the scissile amide bond of the substrate (7). This role requires protonation of Glu73, or more specifically the  $\text{Glu-COO}^- - \text{H}_2\text{O} - \text{Zn}^{2+}$  linkage, in the first step of catalysis. Therefore, it is likely that Glu73 or the Glu73/ $\text{H}_2\text{O}$  system also donates the proton to the amide leaving group in the step that immediately follows to regenerate the basic form

of Glu73 for additional rounds of catalysis (Figure 2). While His253 appears to contribute significantly to catalysis, as shown by the low activity of the H253A mutant, the unchanged pH–rate profile for H253A suggests that it does not act as a catalytic base or acid in the reaction mechanism of LpxC.

Our results indicate that the mechanism of LpxC is like that of other zinc-dependent hydrolases, including carboxypeptidase A (10), leukotriene A4 hydrolase (25), neutral endopeptidase (26), and leucine aminopeptidase (27, 28), that employ a glutamic acid as the catalytic base. Deletion of this critical residue in these other cases results in a protein with little to no discernible activity. While the E73A mutation in LpxC exhibits a loss of activity comparable to the losses of activity of these other general base replacements, the sensitivity of our assay has allowed us to characterize the pH dependence of this mutant, thus providing more direct evidence for the role of Glu73 as the catalytic base. In fact, human matrilysin is the only zinc-dependent hydrolase for which a pH-dependent study following mutation of the conserved active site glutamate has been performed (8). In contrast to our data, the pH–rate profile of the E198A mutant retains the bell-shaped character of that of the wild-type enzyme and discredits the role of Glu198 serving as a catalytic base.

In many well-studied zinc-dependent hydrolases, the concept of general-base-assisted catalysis remains controversial (20, 29). In the case of carbonic anhydrase, for example, zinc-bound hydroxide is expected to exist at neutral pH and therefore act directly as a nucleophile with no assistance by a general-base residue (30). This role requires zinc-bound water to have a sufficiently low  $\text{p}K_a$  to ensure that the hydroxide species exists as the dominant form at neutral pH. Since both the general-base-assisted and zinc hydroxide mechanisms rely on the activation of zinc-bound water, some studies have suggested the preferred mechanistic pathway may be determined by the environment of the  $\text{Zn}^{2+}$  ligand (31). Carbonic anhydrase has three histidine protein ligands, while LpxC has one aspartate and two histidine ligands. A functional study of the  $\text{Zn}^{2+}$  ligand environment in human carbonic anhydrase II showed that substitution of one of the histidine ligands with a negatively charged amino acid increases the  $\text{p}K_a$  of the zinc-bound water by  $\geq 1.6$  pH units (32), demonstrating that neutral ligands maintain a low  $\text{p}K_a$  for zinc-bound water. This suggests that the native  $\text{Zn}^{2+}$  ligand environment in LpxC creates a higher  $\text{p}K_a$  for the zinc-bound water than in carbonic anhydrase and would therefore require deprotonation by a general-base residue, namely, Glu73. Additionally, as the  $\text{p}K_a$  of the zinc-bound water in carbonic anhydrase was found to be 8.4–9.6 following substitution of a  $\text{Zn}^{2+}$  histidine ligand with a carboxylate, it seems likely that  $\text{p}K_2$  in LpxC reflects the ionization of an active zinc-bound water to an inactive zinc-bound hydroxide (see below).

*pH Dependence of Mutants K227A and H253A/K227A.* To investigate the role of other conserved active site residues, particularly regarding  $\text{p}K_2 \approx 8$ , site-directed mutants K227A and H253A/K227A were prepared and their pH-dependent activity was measured. Both the histidine and lysine are located in proximity ( $\sim 4.5$  and  $\sim 5$  Å, respectively) to the zinc-bound water and are only 4 Å from each other. Although the results in Figure 4 appear to demonstrate that His253 is

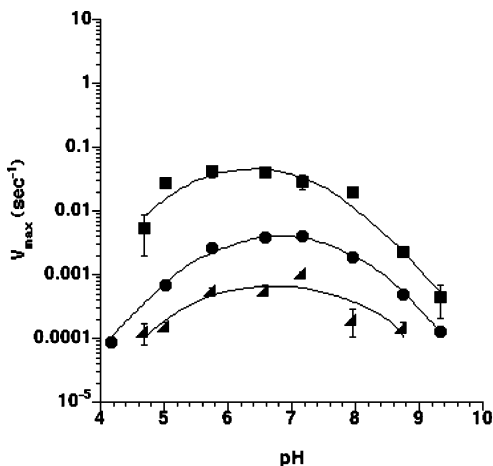


FIGURE 6: pH dependence of  $V_{max}$  for the K227A (circles), H253A/K227A (triangles), and D234N (squares) mutants of LpxC.

not responsible for  $pK_2$ , we entertained the possibility that Lys227 was substituting for His253 somewhat poorly (0.25% activity) yet with approximately the same  $pK_b$  (8 vs 7.8) in the H253A mutant. The pH-dependent  $V_{max}$  profiles of both mutants retain the bell-shaped character seen in the wild-type profile (Figure 6), although both mutants exhibit greatly reduced activity. The K227A mutant has lower activity than H253A with only 0.05% remaining versus the wild type. Its pH-rate profile is very similar to those of both wild-type and H253A, with  $pK_1 = 5.9 \pm 0.1$  and  $pK_2 = 7.8 \pm 0.1$  (Table 1). The double mutant H253A/K227A has only 0.007% remaining activity versus the wild type. Yet even so, its pH dependence also remains bell-shaped with the ionizations  $pK_1 = 5.5 \pm 0.2$  and  $pK_2 = 8.0 \pm 0.2$ . The  $K_M$  remains pH-independent in these mutants since pH-dependent assays performed under  $k_{cat}/K_M$  conditions indicate a bell-shaped profile with similar inflection points (data not shown). As the loss of neither His253 nor Lys227 results in loss of any pH-dependent ionizations, it appears that neither His253 nor Lys227 is responsible for the basic limb of the pH-rate profile. However, the significant loss of activity seen for these mutants does demonstrate that they play important roles in catalysis, perhaps by stabilizing the transition state or organizing the active site through hydrogen bonding. On the basis of the NMR structure, Lys227 is proposed to stabilize the developing negative charge on the oxyanion that forms during catalysis (6). On the basis of the crystal structure, His253 is in a position to hydrogen bond to a nearby aspartate residue (Asp234) or the zinc-bound water (7). Similar roles for basic residues have been reported for other zinc-dependent hydrolases, including a histidine in the neutral protease from *Bacillus subtilis* (33) and an arginine in carboxypeptidase A (9, 21). In contrast to our results following mutagenesis of basic residues, His231 in thermolysin does contribute to the basic limb of the bell-shaped pH-rate profile (34).

**pH Dependence of mutant D234N.** On the basis of the NMR structure, Asp234 is 8 Å from the active site  $Zn^{2+}$  and is expected to hydrogen bond to His253 (6). We investigated the pH dependence of site-directed mutant D234N to define more clearly a role for His253 and/or shed light on the identity of the  $pK_2$  residue. The D234N mutant retains 0.57% residual activity, and the pH dependence of its  $V_{max}$  profile remains bell-shaped (Figure 6). However, with

$pK_1 = 5.5 \pm 0.2$  and  $pK_2 = 7.3 \pm 0.2$  (Table 1) there is a significant shift in  $pK_2$  by >1 pH unit from that of the wild type, while  $pK_1$  remains unchanged (5.5 vs 5.4). Assays performed under  $k_{cat}/K_M$  conditions for this mutant exhibit a similar pH dependence, indicating that  $K_M$  remains pH-independent (data not shown). There have been smaller downward shifts of ~0.5 pH unit in the  $pK_2$  values of some of the other mutants, which we attribute to inaccuracies arising from their low residual activities. Interestingly, the D234N mutant retains the most activity of any mutant tested yet has the greatest deviation from the wild-type profile for  $pK_2$ . This result suggests that Asp234 may be involved in a hydrogen-bonding network in or near the active site that is part of the  $pK_2$  ionization. The shift from  $pK_2 \approx 8.4$  in the wild type to  $pK_2 \approx 7.3$  in the D234N mutant is consistent with the  $pK_2$  residue having a normal ionization closer to 7, e.g., histidine. That is, the perturbed  $pK_2 \approx 8.4$  seen in wild-type LpxC results from its proximity to Asp234. Although His253 is the only conserved histidine in LpxC present in the active site not involved in  $Zn^{2+}$  binding, the H253A data eliminate it as being responsible for  $pK_2$  (Figure 4). We therefore considered the possibility that a different histidine might be acting as the apparent catalytic acid from outside the active site by long-range electrostatics or organization of residues involved in catalysis. We were able to rule out the involvement of all the other histidines in LpxC that do not coordinate  $Zn^{2+}$  with respect to catalytic importance or pH dependence. Two multiple His-replacement mutants were available from related NMR studies that removed all but the most buried (H80) six (H29N, H50A, H55N, H58N, C181A, H188Y, H275\*) or even seven other histidines (previous mutations plus H19N) by site-directed mutagenesis (following paper in this issue). Both of these multiple His mutants retain bell-shaped pH-rate dependence, maintaining 100% or 10% activity, respectively, versus the wild type (data not shown). The  $K_M$  of these mutants remains pH-independent on the basic side of the curve (following paper in this issue). Thus, all other histidine residues have been eliminated as being responsible for the  $pK_2$  ionization.

At this time, no other amino acid residues potentially responsible for the  $pK_2$  ionization have been identified. It is possible that  $pK_2$  arises from a remote network of hydrogen bonds that radiate outward from the active site, as seen in the serine proteases, for example (35). Alternatively, it is possible that  $pK_2$  represents the ionization of the zinc-bound water to zinc-bound hydroxide. This would require zinc-bound hydroxide to be an inactive species, since the activity of LpxC depends on  $pK_2$  being protonated. In accord with this assignment, the predicted  $pK_a$  for zinc-bound water ranges from 8 to 10 (22–24). This is in agreement with the even lower  $pK_a$  of the zinc-bound water ( $pK_a \approx 6.8$ ) in carbonic anhydrase, where three histidine  $Zn^{2+}$  ligands ensure an active zinc-bound hydroxide at neutral pH (32). Further evidence supporting an active zinc-bound water in LpxC comes from NaF inhibition studies, as inhibition by fluoride is a characteristic for enzymes that utilize zinc-bound hydroxide (36, 37). LpxC assayed in the presence of 1–100 mM NaF at pH 5 or 8 shows no inhibition of activity (data not shown). In agreement with  $pK_2$  representing zinc-bound water, disruption of the His253–Asp234 hydrogen bond in the D234N mutant may allow His253 to make a stronger interaction with the carboxylate of Glu73. This could result

in perturbation of the interaction between Glu73 and zinc-bound water and would allow the water to ionize more easily, thus lowering its observed  $pK_a$ . A similar situation has been proposed for a product-bound complex in carboxypeptidase A (38).

## CONCLUSIONS

The experiments presented herein were designed to test the validity of two different proposed mechanisms arising from structural studies of LpxC. Although both mechanisms rely on the activation of zinc-bound water, they differ in the identity of the general base required for its activation. We have demonstrated that the mechanism of LpxC is dependent on two ionizations, one describing protonation of  $pK_1$  and the other involving deprotonation of  $pK_2$ . Although we have not determined the identity of  $pK_2$ , we have provided strong evidence that the first ionization belongs to Glu73. Therefore, deacetylation of UDP-3-*O*-acyl-GlcNAc most likely proceeds via general-base-assisted activation of zinc-bound water by Glu73. This work provides for the first time a direct assignment and measurement of the  $pK_a$  of a general-base residue by a zinc-dependent hydrolase. Future experiments will address the origin of the  $pK_2$  ionization.

## SUPPORTING INFORMATION AVAILABLE

Deconvoluted ESI mass spectra of wild-type AaLpxC and its variants. This material is available free of charge via the Internet at <http://pubs.acs.org>.

## REFERENCES

- Raetz, C. R., and Whitfield, C. (2002) Lipopolysaccharide endotoxins, *Annu. Rev. Biochem.* 71, 635–700.
- Clements, J. M., Coignard, F., Johnson, I., Chandler, S., Palan, S., Waller, A., Wijkman, J., and Hunter, M. G. (2002) Antibacterial activities and characterization of novel inhibitors of LpxC, *Antimicrob. Agents Chemother.* 46, 1793–1799.
- Jackman, J. E., Fierke, C. A., Tumey, L. N., Pirrung, M., Uchiyama, T., Tahir, S. H., Hindsgaul, O., and Raetz, C. R. (2000) Antibacterial agents that target lipid A biosynthesis in gram-negative bacteria. Inhibition of diverse UDP-3-*O*-(*r*-3-hydroxymyristoyl)-*n*-acetylglucosamine deacetylases by substrate analogs containing zinc binding motifs, *J. Biol. Chem.* 275, 11002–11009.
- Kline, T., Andersen, N. H., Harwood, E. A., Bowman, J., Malanda, A., Endsley, S., Erwin, A. L., Doyle, M., Fong, S., Harris, A. L., Mendelsohn, B., Mdluli, K., Raetz, C. R., Stover, C. K., Witte, P. R., Yabannavar, A., and Zhu, S. (2002) Potent, novel in vitro inhibitors of the *Pseudomonas aeruginosa* deacetylase LpxC, *J. Med. Chem.* 45, 3112–3129.
- Onishi, H. R., Pelak, B. A., Gerckens, L. S., Silver, L. L., Kahan, F. M., Chen, M. H., Patchett, A. A., Galloway, S. M., Hyland, S. A., Anderson, M. S., and Raetz, C. R. (1996) Antibacterial agents that inhibit lipid A biosynthesis, *Science* 274, 980–982.
- Coggins, B. E., Li, X., McClerren, A. L., Hindsgaul, O., Raetz, C. R., and Zhou, P. (2003) Structure of the LpxC deacetylase with a bound substrate-analog inhibitor, *Nat. Struct. Biol.* 10, 645–651.
- Whittington, D. A., Rusche, K. M., Shin, H., Fierke, C. A., and Christianson, D. W. (2003) Crystal structure of LpxC, a zinc-dependent deacetylase essential for endotoxin biosynthesis, *Proc. Natl. Acad. Sci. U.S.A.* 100, 8146–8150.
- Cha, J., and Auld, D. S. (1997) Site-directed mutagenesis of the active site glutamate in human matrilysin: investigation of its role in catalysis, *Biochemistry* 36, 16019–16024.
- Christianson, D. W., and Lipscomb, W. N. (1989) Carboxypeptidase A, *Acc. Chem. Res.* 22, 62–69.
- Lipscomb, W. N., and Strater, N. (1996) Recent Advances in Zinc Enzymology, *Chem. Rev.* 96, 2375–2434.
- Matthews, B. W. (1988) Structural basis of the action of Thermolysin and related zinc peptidases, *Acc. Chem. Res.* 21, 333–340.
- Jackman, J. E., Raetz, C. R., and Fierke, C. A. (2001) Site-directed mutagenesis of the bacterial metalloamidase UDP-(3-*O*-acyl)-*N*-acetylglucosamine deacetylase (LpxC). Identification of the zinc binding site, *Biochemistry* 40, 514–523.
- Finnin, M. S., Donigian, J. R., Cohen, A., Richon, V. M., Rifkind, R. A., Marks, P. A., Breslow, R., and Pavletich, N. P. (1999) Structures of a histone deacetylase homologue bound to the TSA and SAHA inhibitors, *Nature* 401, 188–193.
- Jackman, J. E., Raetz, C. R., and Fierke, C. A. (1999) UDP-3-*O*-(*R*-3-hydroxymyristoyl)-*N*-acetylglucosamine deacetylase of *Escherichia coli* is a zinc metalloenzyme, *Biochemistry* 38, 1902–1911.
- Fersht, A. (1999) *Structure and mechanism in protein science*, W. H. Freeman and Co., New York.
- Cleland, W. W. (1979) Statistical analysis of enzyme kinetic data, *Methods Enzymol.* 63, 103–138.
- Auld, D. S., and Vallee, B. L. (1970) Kinetics of carboxypeptidase A. The pH dependence of tripeptide hydrolysis catalyzed by zinc, cobalt, and manganese enzymes, *Biochemistry* 9, 4352–4359.
- Breslow, R., and Wernick, D. L. (1977) Unified picture of mechanisms of catalysis by carboxypeptidase A, *Proc. Natl. Acad. Sci. U.S.A.* 74, 1303–1307.
- Mock, W. L., and Stanford, D. J. (1996) Arazoformyl dipeptide substrates for thermolysin. Confirmation of a reverse protonation catalytic mechanism, *Biochemistry* 35, 7369–7377.
- Makinen, M., Wells, G., and Kang, S. (1984) in *Advances in Inorganic Biochemistry* (Eichhorn, G., and Marzilli, L., Eds.) pp 1–49, Elsevier, New York.
- Phillips, M. A., Fletterick, R., and Rutter, W. J. (1990) Arginine 127 stabilizes the transition state in carboxypeptidase, *J. Biol. Chem.* 265, 20692–20698.
- Baes, C. F., and Messmer, R. E. (1976) *The hydrolysis of cations*, Wiley-Interscience, New York.
- Basolo, and Pearson (1967) *Mechanisms of inorganic reactions*, 2nd ed., Wiley, New York.
- Woolley, P. (1975) Models for metal ion function in carbonic anhydrase, *Nature* 258, 677–682.
- Wetterholm, A., Medina, J. F., Radmark, O., Shapiro, R., Haeggstrom, J. Z., Vallee, B. L., and Samuelsson, B. (1992) Leukotriene A4 hydrolase: abrogation of the peptidase activity by mutation of glutamic acid-296, *Proc. Natl. Acad. Sci. U.S.A.* 89, 9141–9145.
- Devault, A., Nault, C., Zollinger, M., Fournie-Zaluski, M. C., Roques, B. P., Crine, P., and Boileau, G. (1988) Expression of neutral endopeptidase (enkephalinase) in heterologous COS-1 cells. Characterization of the recombinant enzyme and evidence for a glutamic acid residue at the active site, *J. Biol. Chem.* 263, 4033–4040.
- Bzymek, K. P., and Holz, R. C. (2004) The catalytic role of glutamate 151 in the leucine aminopeptidase from *Aeromonas proteolytica*, *J. Biol. Chem.* 279, 31018–31025.
- Bienvenue, D. L., Mathew, R. S., Ringe, D., and Holz, R. C. (2002) The aminopeptidase from *Aeromonas proteolytica* can function as an esterase, *J. Biol. Inorg. Chem.* 7, 129–135.
- Bounaga, S., Laws, A. P., Galleni, M., and Page, M. I. (1998) The mechanism of catalysis and the inhibition of the *Bacillus cereus* zinc-dependent beta-lactamase, *Biochem. J.* 331 (Part 3), 703–711.
- Silverman, D. N., and Lindskog, S. (1988) The catalytic mechanism of Carbonic Anhydrase: implications of a rate-limiting protolysis of water, *Acc. Chem. Res.* 21, 30–36.
- Vallee, B. L., and Auld, D. S. (1990) Active-site zinc ligands and activated H<sub>2</sub>O of zinc enzymes, *Proc. Natl. Acad. Sci. U.S.A.* 87, 220–224.
- Kiefer, L. L., and Fierke, C. A. (1994) Functional characterization of human carbonic anhydrase II variants with altered zinc binding sites, *Biochemistry* 33, 15233–15240.
- Toma, S., Campagnoli, S., De Gregoriis, E., Gianna, R., Margarit, I., Zamai, M., and Grandi, G. (1989) Effect of Glu-143 and His-231 substitutions on the catalytic activity and secretion of *Bacillus subtilis* neutral protease, *Protein Eng* 2, 359–364.
- Beaumont, A., O'Donohue, M. J., Paredes, N., Rouselet, N., Assicot, M., Bohuon, C., Fournie-Zaluski, M. C., and Roques, B. P. (1995) The role of histidine 231 in thermolysin-like enzymes. A site-directed mutagenesis study, *J. Biol. Chem.* 270, 16803–16808.

35. Hedstrom, L. (2002) Serine protease mechanism and specificity, *Chem. Rev.* 102, 4501–4524.
36. Chen, G., Edwards, T., D'Souza V, M., and Holz, R. C. (1997) Mechanistic studies on the aminopeptidase from *Aeromonas proteolytica*: a two-metal ion mechanism for peptide hydrolysis, *Biochemistry* 36, 4278–4286.
37. Harris, M. N., and Ming, L. J. (1999) Different phosphate binding modes of *Streptomyces griseus* aminopeptidase between crystal and solution states and the status of zinc-bound water, *FEBS Lett.* 455, 321–324.
38. Zhang, K., and Auld, D. S. (1993) XAFS studies on carboxypeptidase A: Detection of a structural alteration in the zinc coordination sphere coupled to the catalytically important alkaline pK<sub>a</sub>, *Biochemistry* 32, 13844–13851.
39. Koradi, R., Billeter, M., and Wuthrich, K. (1996) MOLMOL: A program for display and analysis of macromolecular structures, *J. Mol. Graphics* 14, 29–32, 51–55.

BI048001H